ChemComm

COMMUNICATION

View Article Online
View Journal | View Issue

Cite this: *Chem. Commun.*, 2026, **62**, 3269

Received 26th November 2025,
Accepted 8th January 2026

DOI: 10.1039/d5cc06700f

rsc.li/chemcomm

When gold and silver differ: interactions of N-heterocyclic carbenes with noble metal surfaces

Aruna Chandran, †[a] Shayanta Chowdhury, †[a] Gurkiran Kaur, [b] Gaohe Hu,[c] Nathaniel L. Dominique, [a] Lasse Jensen, *[c] David M. Jenkins *[b] and Jon P. Camden *[a]

N-heterocyclic carbenes have transformed gold surface chemistry, but conventional deposition methods do not always translate effectively to silver substrates. We introduce a benchtop protocol that yields comparable monolayers on both metals, but also etches silver during the process. Controls show that oxygen is essential in both monolayer formation and substrate etching.

N-heterocyclic carbenes (NHCs) are generating significant interest as surface functionalization ligands, further expanding on their already impressive catalytic capabilities for alkene metathesis and cross-coupling reactions.[1] NHCs are now recognized as excellent surface passivation agents for gold surfaces and nanoparticles, combining exceptionally strong adhesion with modularity in a way that other stabilizing ligands, such as phosphines and thiols, do not.[2] This newly expanded application space is driving intense interest in elucidating the interaction, binding, self-assembly, and stability of NHCs on gold.[3–5]

Despite being one row above gold on the periodic table, reports of NHC self-assembled monolayers (SAMs) on silver substrates remain rare.[6–14] This stands in contrast to thiols, which are the dominant ligand for functionalization of noble metal surfaces and display very similar behavior on gold and silver substrates.[15–18] Of particular note, the few studies exploring the deposition of NHCs on silver surfaces utilize ultra-high vacuum (UHV)[6,7] or electrochemical deposition.[9] While these methods are effective, the applicability of Ag-NHC SAMs would be greatly expanded by the development of a solution-based benchtop approach similar to those available for gold.[19–21] In this work, we explore whether established benchtop protocols for NHC monolayer formation on gold surfaces can be extended to silver. Remarkably, we find significant differences between the monolayers formed *via* the same methods on gold and silver surfaces, revealing an unexpected divergence in NHC surface chemistry between the two coinage metals.

Specifically, we report the deposition of diisopropyl benzimidazolium carbene on silver substrates using a 24-hour methanolic deposition starting from the CO_2-adducts (**NHC-CO_2**) at 58 °C under benchtop conditions (Fig. 1A and B).[19] This method is found to apply to both gold and silver surfaces. Characterization by surface-enhanced Raman scattering (SERS) and laser-desorption ionization mass spectrometry (LDI-MS) indicated similar SAM formation, while scanning electron

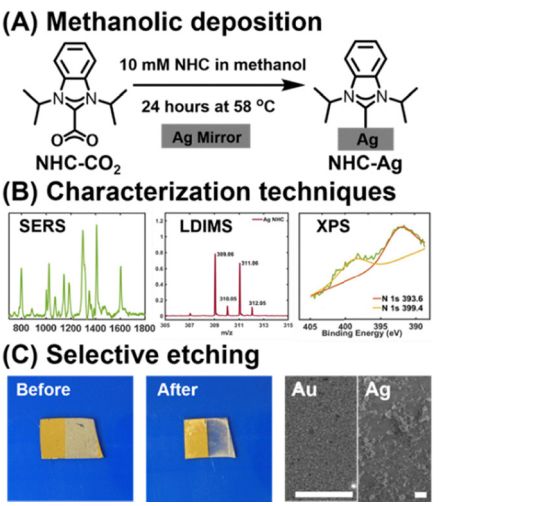

Fig. 1 Schematic overview of NHC monolayer deposition and characterization. (A) NHC SAM deposited on Ag surface using a 24-hour heated methanolic deposition. (B) The NHC monolayers were characterized using surface-enhanced Raman spectroscopy (SERS), laser desorption/ionization mass spectrometry (LDI-MS), and X-ray photoelectron spectroscopy (XPS). (C) Selective etching of Ag (right) but not Au (left) under heated methanolic deposition conditions, along with the scanning electron microscopy (SEM) images of Au and Ag substrates.

[a] *Department of Chemistry and Biochemistry, University of Notre Dame, Notre Dame, IN 46556, USA. E-mail: jon.camden@nd.edu*
[b] *Department of Chemistry, University of Tennessee, Knoxville, TN 37996, USA. E-mail: djenki15@utk.edu*
[c] *Department of Chemistry, The Pennsylvania State University, University Park, PA 16802, USA. E-mail: lxj18@psu.edu*
† These authors contributed equally.

microscopy (SEM) revealed a significant etching of the silver surface (Fig. 1C). When both gold and silver were present, the silver was selectively etched over gold, although gold etching was observed at very long times. Surprisingly, oxygen was found to be a key component in the deposition procedure, and no deposition or etching occurred on silver in the absence of oxygen.

To provide a detailed comparison between gold and silver NHC surfaces prepared according to this method, we performed SERS, LDI-MS, and X-ray photoelectron spectroscopy (XPS). Fig. 2 compares the SERS spectra of **NHC-CO_2** deposited on silver and gold film-over-nanosphere (FON) substrates. While the spectra are largely similar, shifts in the bands near $\sim$800 cm^{-1}, $\sim$1295 cm^{-1}, and $\sim$1405 cm^{-1} (highlighted in red in Fig. 2, top) were observed. These same vibrational modes shift when the carbene carbon is isotope labeled (Fig. 2, bottom), and these vibrational modes are diagnostic for the metal-NHC bond.[22,23] These normal modes involve local metal-carbene bond motion and, therefore, substituting Ag for Au is expected to shift the same peaks affected by the carbon isotope-labeling. Notably, the modes unaffected by isotope substitution also remain unchanged between Ag and Au. Computational simulations support this conclusion, as NHCs bound to Au and Ag exhibit analogous shifts in frequency (Fig. S1). The similarity in the experimental and simulated SERS is also an indication that the binding motif of NHC SAMs on silver is similar to that of gold with this deposition protocol.

Interestingly, the other standard gold NHC-functionalization methods, like the free carbene deposition from **[(NHC-H)PF_6]** and the heated methanolic deposition of **[(NHC-H)HCO_3]**,[19] failed to produce identical monolayers on silver, as observed *via* SERS (Fig. S2). Both methods resulted in additional peaks appearing near $\sim$785 cm^{-1}, $\sim$1312 cm^{-1}, and $\sim$1430 cm^{-1}, which likely indicate the presence of physisorbed species.[19] Low vacuum annealing with **NHC-CO_2** at different temperatures resulted in SERS spectra with no suggestions of monolayer formation (Fig. S2).

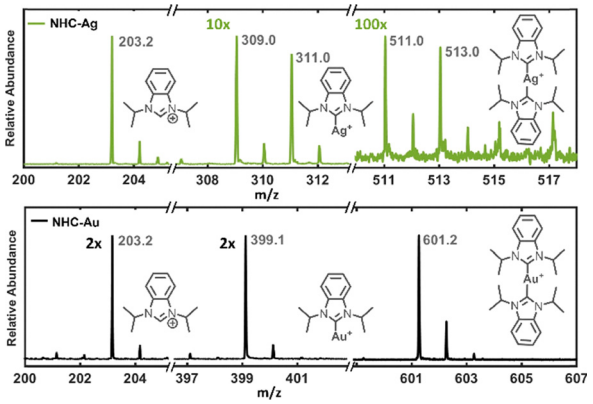

Fig. 3 LDI-MS of NHC-Ag/Au monolayers. NHC deposited on Ag (green) and Au (black) mirrors are characterized with LDI-MS, and NHC ion channels corresponding to **[NHC-H]$^+$**, **[(NHC)Ag]$^+$**, and **[$(NHC)_2$Ag]$^+$** are displayed.

LDI-MS is widely used for probing SAMs on metal surfaces, and it has become a standard way to characterize NHC monolayers on gold.[24–28] Fig. 3 compares the LDI spectra obtained from NHCs on gold and silver substrates, focusing on three regions of the mass spectra: (1) the **[NHC-H]$^+$** cation, (2) the mono **[(NHC)Ag]$^+$** ion, and (3) the bis **[$(NHC)_2$Ag]$^+$** ion. The presence of the mono- and bis-ions supports the chemisorption of NHCs on the silver surface, and the bis-ion suggests that the NHCs are sufficiently closely packed to allow for bis-ion formation during the desorption process.[24]

We observed a notable difference in signal intensity when comparing the **NHC-Ag** and **NHC-Au** systems. In the silver

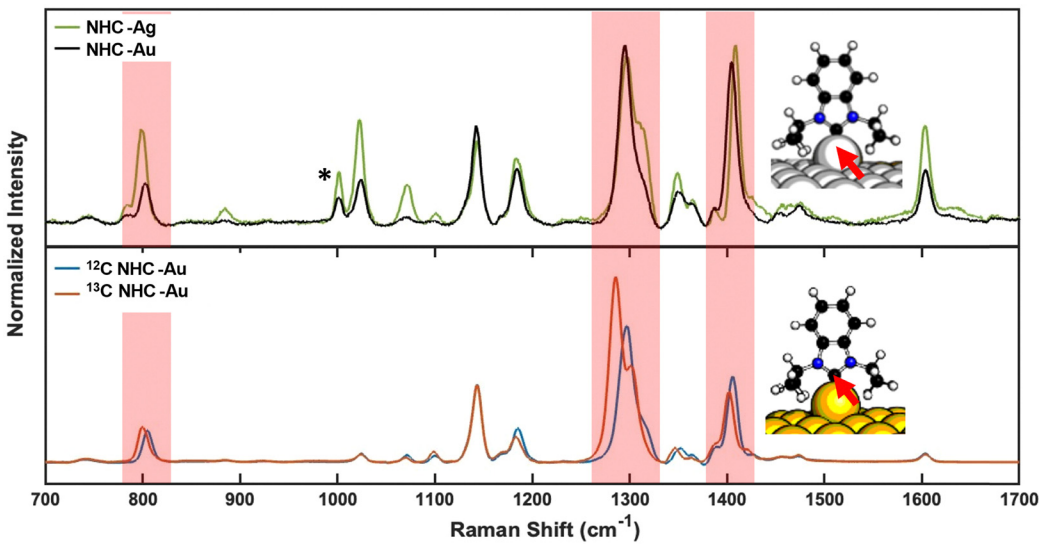

Fig. 2 SERS of NHC-Ag/Au monolayers. Top: SERS of NHC deposited on the Ag surface (green) is overlaid with NHC deposited on Au (black) using the procedure given in Fig. 1A. Bottom: SERS of ^{13}C-labelled NHC (red) and ^{12}C-NHC (blue) on Au nanoparticles. The highlighted regions (red) indicate peak shifts consistent with isotopic shifts (bottom panel) observed for ^{13}C-labelled NHC bound to Au. Asterisks indicate the mode from polystyrene beads below the Au or Ag film. Data on the bottom panel is reproduced from ref. 21.

system, the bis $[(NHC)_2Ag]^+$ ion signal for Ag-NHC was approximately 10 times less intense than the mono $[(NHC)Ag]^+$ ion. In contrast, the **NHC-Au** monolayer exhibited a bis $[(NHC)_2Au]^+$ ion signal roughly twice as intense as the mono $[(NHC)Au]^+$ signal. This difference in the intensities of mono- and bis-NHC ions can be attributed firstly to the metal-NHC bond strength.[29,30] The bond dissociation energy for NHCs to gold is $\sim$27 kcal mol^{-1} stronger than silver, which, when combined with the strong *trans* influence of NHCs,[31] may cause the bis $[(NHC)_2Ag]^+$ ion to be less favorable compared to gold. Secondly, reports have shown that adatoms are possible on silver surfaces, similar to that of gold.[6,8,12] However, the adatom formation and the resulting binding motif for the UHV method depends on experimental conditions like deposition temperature, surface structure and coverage.[6,12] Therefore, it is possible that our method produces NHCs that are not packed as tightly across the silver surface, which would reduce the possibility of forming bis-NHC metal ions upon excitation. Further studies, which are beyond the scope of this initial report, would be required to elucidate the details of the LDI spectra.

XPS is commonly used to confirm the chemisorption of NHC monolayers on gold, with a shift in the N1s peak typically appearing between 399.9 and 401.0 eV binding energy (Fig. S5B).[32–35] For NHCs bound to silver, signals in this region have been reported as N1s peaks confirming monolayer formation.[9] However, in control experiments performed in the absence of NHCs, we find the same two peaks (Fig. S5C). The feature at 399.3 eV corresponds to the energy losses from the Ag $3d_{5/2}$ peak, and the feature at 393.9 eV from the Ag $3d_{3/2}$ peak.[36] For the **NHC-Ag** samples, we find the signals to be nearly identical to the control (Fig. S5D); therefore, in case of silver substrates, we find XPS to be inconclusive, and recommend the use of other methods for confirmation.

Unlike gold, significant etching of the silver surface is observed with heated methanolic NHC deposition (Fig. 4). This behavior is consistent with prior reports, which show that NHCs can also etch gold under certain conditions.[37,38] Introducing a large excess of NHCs to gold nanoparticles also results in etching and subsequent formation of soluble NHC gold complexes, destabilizing the nanostructures in the process.[39]

To compare the etching behavior between silver and gold, we prepared five different metal-mirror substrates, shown schematically in Fig. 4A and Fig. S6. Fig. 4B shows the photographs and SEM images of the control mirrors exposed to heated methanolic conditions in the absence of NHC, while the corresponding images in the presence of NHCs are shown in Fig. 4C. SEM analysis revealed an increase in grain size after 24 hours of methanolic NHC deposition, along with the appearance of dark spots that are absent in the blank silver mirror sample. These dark spots indicate the formation of surface holes, resulting from the NHC-induced etching of the silver surface. In mirrors constructed with Ag atop Au, selective removal of the silver layer was observed after 24 hours, exposing the underlying gold layer. EDX analysis of these samples confirmed the presence of small residual silver grains on the gold surface (Fig. S7), which appeared brighter in SEM due to their higher elevation relative to the gold layer. In the case of Ag/Au striped mirrors, the silver regions were selectively etched by the NHC treatment, exposing the underlying glass substrate. SEM images showed little to no silver remaining on these samples, while the Au surface exhibited minimal etching

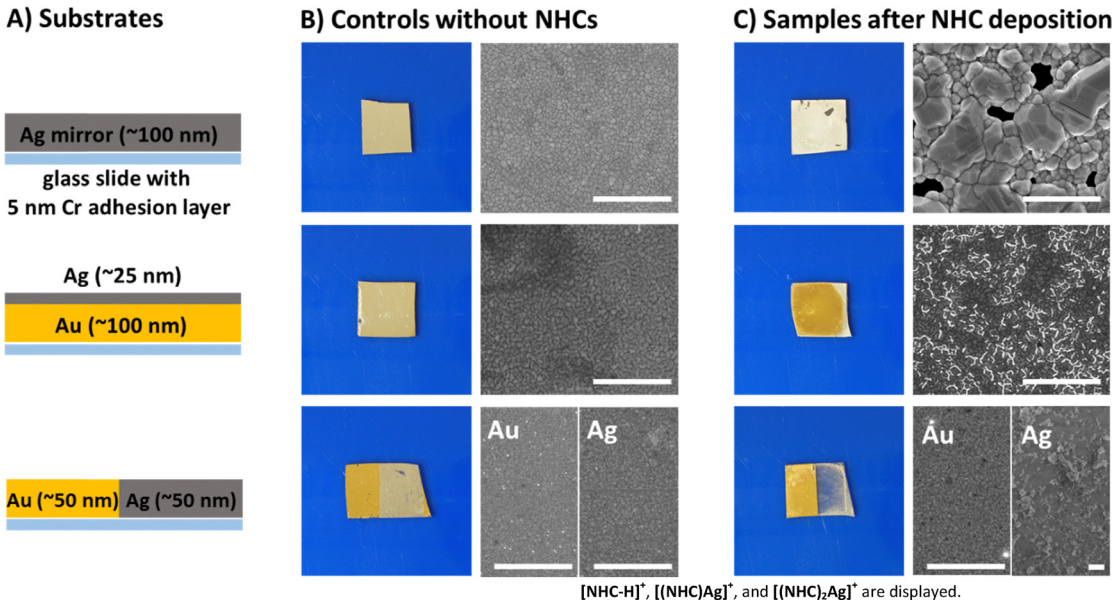

Fig. 4 SEM of NHCs deposited on Ag and Au substrates. (A) Ag and Au mirror substrates. Photographic and SEM images of mirror substrates subjected to heated methanolic deposition without (B) and with (C) the presence of NHCs. The SEM images confirm the selective etching of Ag surfaces under heated methanolic deposition conditions. The length of the scale bars represents 1 μm.

(Fig. 4C). For the bilayer mirrors with Au atop Ag, the etching of the underlying silver led to delamination of the Au layer. Collectively, these experiments demonstrate that NHCs selectively etch silver surfaces while exhibiting negligible etching towards Au. This selectivity is likely due to the differences in the metal-carbene bonding between **NHC-Ag** and **NHC-Au**, as well as the higher reactivity and lower reduction potential of silver compared to gold. While the silver layer is heavily etched *via* this procedure, there is also evidence of the beginning of etching on the Au layer, albeit at a much slower rate. When a gold substrate was subjected to 2 weeks of methanolic NHC deposition, SEM revealed surface holes and a change in morphology (Fig. S8).

To further investigate the mechanism of this etching behavior of NHCs on silver, we conducted a series of experiments involving nitrogen degassing of the methanolic solution followed by oxygen bubbling. The corresponding SERS and LDI-MS data are shown in Fig. S9 and Fig. S10, respectively. Nitrogen degassing removed dissolved oxygen from the methanol, and under these conditions, no peaks were observed for SERS as well as LDI-MS, showing an absence of NHC monolayer formation. However, when oxygen was reintroduced to the methanolic solution and the deposition procedure repeated, the characteristic SERS and LDI-MS peaks for NHCs were detected. These results suggest that oxygen plays a crucial role in methanolic deposition and subsequent etching processes.

In conclusion, this work demonstrates a benchtop method of depositing the standard diisopropyl benzimidazolium carbene on silver surfaces that produces a comparable SAM to that on gold. XPS determination of NHC chemisorption on silver is ineffective due to the presence of Ag 3d loss peaks in the key NHC N 1s region, which results in an NHC monolayer and a silver blank presenting similar spectral features. SEM characterization further reveals selective etching of silver under these deposition conditions, indicating different surface reactivity of silver towards NHCs compared to gold. The selective etching also creates avenues for gold recycling and the synthesis of nanoporous gold and other gold nanostructures using NHCs, with the added benefit of sustainability and biocompatibility.[38,40] The presence of oxygen is found to be crucial for NHC deposition and etching on both gold and silver surfaces. Overall, these findings suggest that, unlike thiols, which are known to interact similarly with both metals, NHCs exhibit distinct surface chemistry on gold and silver, depending on the deposition conditions.

This work was supported by the National Science Foundation under Grants CHE-2404020 (A. C., S. C., and J. P. C.), CHE-2404021 (G. K. and D. M. J.), and CHE-2312222 (G. H. and L. J.). The content is solely the responsibility of the authors and does not necessarily represent the official views of the National Science Foundation. A. C. thanks William Boggess of the Notre Dame Mass Spectrometry and Proteomics facility for the use of the Bruker Ultraflextreme MALDI-TOF mass spectrometer, Tatyana Orlova for the use of the field emission scanning electron microscope (FESEM), and Douglas Miller for his assistance in setting up the oxygen gas bubbling experiment.

Conflicts of interest

There are no conflicts to declare.

Data availability

The data supporting this article have been included as part of the supplementary information (SI). Supplementary information: the supplementary information includes materials, experimental details, computational details, SERS, LDI-MS, XPS, NMR spectra, and SEM images. See DOI: https://doi.org/10.1039/d5cc06700f.

References

1 M. Koy, P. Bellotti, M. Das and F. Glorius, *Nat. Catal.*, 2021, **4**, 352–363.
2 C. A. Smith, M. R. Narouz, P. A. Lummis, I. Singh, A. Nazemi, C.-H. Li and C. M. Crudden, *Chem. Rev.*, 2019, **119**, 4986–5056.
3 G. Kaur, R. L. Thimes, J. P. Camden and D. M. Jenkins, *Chem. Commun.*, 2022, **58**, 13188–13197.
4 P. Bellotti, M. Koy, M. N. Hopkinson and F. Glorius, *Nat. Rev. Chem.*, 2021, **5**, 711–725.
5 T. Weidner, J. E. Baio, A. Mundstock, C. Große, S. Karthäuser, C. Bruhn and U. Siemeling, *Aust. J. Chem.*, 2011, **64**, 1177–1179.
6 L. Jiang, B. Zhang, G. Médard, A. P. Seitsonen, F. Haag, F. Allegretti, J. Reichert, B. Kuster, J. V. Barth and A. C. Papageorgiou, *Chem. Sci.*, 2017, **8**, 8301–8308.
7 A. Bakker, M. Freitag, E. Kolodzeiski, P. Bellotti, A. Timmer, J. Ren, B. Schulze Lammers, D. Moock, H. W. Roesky, H. Mönig, S. Amirjalayer, H. Fuchs and F. Glorius, *Angew. Chem., Int. Ed.*, 2020, **59**, 13643–13646.
8 J. Ren, M. Freitag, C. Schwermann, A. Bakker, S. Amirjalayer, A. Rühling, H.-Y. Gao, N. L. Doltsinis, F. Glorius and H. Fuchs, *Nano Lett.*, 2020, **20**, 5922–5928.
9 E. Amit, L. Dery, S. Dery, S. Kim, A. Roy, Q. Hu, V. Gutkin, H. Eisenberg, T. Stein, D. Mandler, F. D. Toste and E. Gross, *Nat. Commun.*, 2020, **11**, 5714.
10 J. Ren, M. Das, Y. Gao, A. Das, A. H. Schäfer, H. Fuchs, S. Du and F. Glorius, *J. Am. Chem. Soc.*, 2024, **146**, 32558–32566.
11 L. Li, S. Mahapatra, J. F. Schultz, X. Zhang and N. Jiang, *ACS Nano*, 2024, **18**, 32118–32125.
12 L. Li, J. F. Schultz, S. Mahapatra, D. Liu, X. Zhang and N. Jiang, *ACS Nano*, 2025, **19**, 15363–15370.
13 S. Mahapatra, L. Li and N. Jiang, *ChemPhysChem*, 2025, 2500227.
14 L. Zhang, Z. Liu, Y. Zhang, X. Xu and Y. Tang, *Mater. Chem. Phys.*, 2025, 131322.
15 M. A. Bryant and J. E. Pemberton, *J. Am. Chem. Soc.*, 1991, **113**, 8284–8293.
16 H. T. Rong, S. Frey, Y. J. Yang, M. Zharnikov, M. Buck, M. Wühn, C. Wöll and G. Helmchen, *Langmuir*, 2001, **17**, 1582–1593.
17 S. Frey, V. Stadler, K. Heister, W. Eck, M. Zharnikov, M. Grunze, B. Zeysing and A. Terfort, *Langmuir*, 2001, **17**, 2408–2415.
18 F. Sun, D. D. Galvan, P. Jain and Q. Yu, *Chem. Commun.*, 2017, **53**, 4550–4561.
19 A. Chandran, N. L. Dominique, G. Kaur, V. Clark, P. Nalaoh, L. C. Ekowo, I. M. Jensen, M. D. Aloisio, C. M. Crudden, N. Arroyo-Currás, D. M. Jenkins and J. P. Camden, *Nanoscale*, 2025, **17**, 5413–5428.
20 M. A. Pellitero, I. M. Jensen, N. L. Dominique, L. C. Ekowo, J. P. Camden, D. M. Jenkins and N. Arroyo-Currás, *ACS Appl. Mater. Interfaces*, 2023, **15**, 35701–35709.
21 C. Gutheil, G. Roß, S. Amirjalayer, B. Mo, A. H. Schäfer, N. L. Doltsinis, B. R. Braunschweig and F. Glorius, *ACS Nano*, 2024, **18**, 3043–3052.
22 S. Chowdhury, G. Hu, I. M. Jensen, A. V. Santos, D. M. Jenkins, L. Jensen and J. P. Camden, *J. Phys. Chem. C*, 2024, **128**, 13550–13557.
23 I. M. Jensen, S. Chowdhury, G. Hu, L. Jensen, J. P. Camden and D. M. Jenkins, *Chem. Commun.*, 2023, **59**, 14524–14527.

24 N. L. Dominique, S. L. Strausser, J. E. Olson, W. C. Boggess, D. M. Jenkins and J. P. Camden, *Anal. Chem.*, 2021, **93**, 13534–13538.
25 M. Mrksich, *ACS Nano*, 2008, **2**, 7–18.
26 N. L. Dominique, I. M. Jensen, G. Kaur, C. Q. Kotseos, W. C. Boggess, D. M. Jenkins and J. P. Camden, *Angew. Chem., Int. Ed.*, 2023, **62**, e202219182.
27 Z. A. Gurard-Levin, M. D. Scholle, A. H. Eisenberg and M. Mrksich, *ACS Comb. Sci.*, 2011, **13**, 347–350.
28 N. L. Dominique, R. Chen, A. V. Santos, S. L. Strausser, T. Rauch, C. Q. Kotseos, W. C. Boggess, L. Jensen, D. M. Jenkins and J. P. Camden, *Inorg. Chem. Front.*, 2022, **9**, 6279–6287.
29 C. Boehme and G. Frenking, *Organometallics*, 1998, **17**, 5801–5809.
30 L. Kuster, M. Bélanger-Bouliga, T. E. Shaw, A. Nazemi and M. Frenette, *Nanoscale*, 2024, **16**, 11052–11068.
31 S. Fuertes, A. s J. Chueca and V. Sicilia, *Inorg. Chem.*, 2015, **54**, 9885–9895.
32 A. Bakker, A. Timmer, E. Kolodzeiski, M. Freitag, H. Y. Gao, H. Mönig, S. Amirjalayer, F. Glorius and H. Fuchs, *J. Am. Chem. Soc.*, 2018, **140**, 11889–11892.
33 E. A. Doud, R. L. Starr, G. Kladnik, A. Voevodin, E. Montes, N. P. Arasu, Y. Zang, P. Zahl, A. Morgante, L. Venkataraman, H. Vázquez, D. Cvetko and X. Roy, *J. Am. Chem. Soc.*, 2020, **142**, 19902–19906.
34 J. Ren, M. Freitag, Y. Gao, P. Bellotti, M. Das, B. Schulze Lammers, H. Mönig, Y. Zhang, C. G. Daniliuc, S. Du, H. Fuchs and F. Glorius, *Angew. Chem., Int. Ed.*, 2022, **61**, e202115104.
35 A. Inayeh, R. R. Groome, I. Singh, A. J. Veinot, F. C. de Lima, R. H. Miwa, C. M. Crudden and A. B. McLean, *Nat. Commun.*, 2021, **12**, 4034.
36 N. Pauly, F. Yubero and S. Tougaard, *Appl. Surf. Sci.*, 2016, **383**, 317–323.
37 S. Zhou, D. Huo, S. Goines, T.-H. Yang, Z. Lyu, M. Zhao, K. D. Gilroy, Y. Wu, Z. D. Hood, M. Xie and Y. Xia, *J. Am. Chem. Soc.*, 2018, **140**, 11898–11901.
38 R. B. Chevalier, J. Pantano, M. K. Kiesewetter and J. R. Dwyer, *Beilstein J. Nanotechnol.*, 2023, **14**, 865–871.
39 N. A. Nosratabad, Z. Jin, H. Arabzadeh, B. Chen, C. Huang and H. Mattoussi, *Dalton Trans.*, 2024, **53**, 467–483.
40 A. Zupanc, J. Install, M. Jereb and T. Repo, *Angew. Chem., Int. Ed.*, 2023, **62**, e202214453.